Int J Clin Exp Pathol 2026;19(7):324-339
www.ijcep.com /ISSN:1936-2625/IJCEP0169998

Original Article

PDGFRA mediates the PI3K/AKT signaling pathway to regulate the growth and phenotype of GCTB tumor cells

Tiantian Zhang[1*], Wanjing Song[1*], Zhengqing Yan[1,2], Zhonghua Zhao[1], Zhongqing Chen[3], Feng Tang[3], Kanda Gao[4], Feiyan Chen[4], Hongguang Zhu[1], Shuyang Wang[1,5]

[1]Department of Pathology, School of Basic Medicine, Fudan University, Shanghai, China; [2]Department of General Surgery, Huashan Hospital Affiliated to Fudan University, Shanghai, China; [3]Department of Pathology, Huashan Hospital Affiliated to Fudan University, Shanghai, China; [4]Department of Orthopedics, Huashan Hospital Affiliated to Fudan University, Shanghai, China; [5]Shanghai Key Laboratory of Medical Imaging Computing and Computer Assisted Intervention, Shanghai, China. [*]Equal contributors.

Received November 14, 2025; Accepted June 23, 2026; Epub July 15, 2026; Published July 30, 2026

Abstract: Purpose: The nature of true neoplastic cells of giant cell tumor of bone (GCTB) remains unverified. As the effect of denosumab on true neoplastic cells needs to be clarified, direct targeting of these cells remains unclear. Methods: In this study, we obtained 32 formalin-fixed paraffin-embedded (FFPE) GCTB tissue blocks, performing H&E staining and immunohistochemistry staining of CD68. Multinucleated giant cells, monocytes, and CD68-negative mononuclear spindle cells were accurately captured by laser capture microdissection. The DNA of these cells was extracted, digested with *Hpa*II and subjected to nested PCR amplification. We isolated and cultured GCTB primary tumor cells. The primary tumor cells were treated with denosumab and PDGFRA inhibitors. CCK8 assays and RT-qPCR were performed to reveal the effect of the inhibitors. Results: In *HUMARA*-heterozygous samples, CD68 negative mononuclear spindle cells appeared as only one main peak after digestion, which suggests that the CD68 negative mononuclear spindle cells are monoclonal. Denosumab had no direct effect on the growth of GCTB primary tumor cells. PDGFRA inhibitor Avapritinib had a direct inhibitory effect on the growth of the tumor cells and altered the tumor cell phenotype. AKT inhibitors had a similar inhibitory effect as Avapritinib. Avapritinib altered the expression of AKT-related genes, and down-regulated pGSK3β. The downregulation of pAKT and pGSK3β was partially reversed by co-treatment with the AKT agonist SC79, suggesting PI3K/AKT as a downstream pathway of PDGFRA. Conclusion: CD68 negative mononuclear spindle cells are the true neoplastic cells of GCTB. PDGFRA inhibition may be a novel targeted therapy for GCTB.

Keywords: Giant cell tumor of bone, clonality analysis, PDGFRA

Introduction

Giant cell tumor of bone (GCTB) is a primary borderline bone tumor, which typically occurs in the epiphysis of long bones, such as the distal femur, proximal tibia, and distal radius, etc. [1]. The main clinical symptoms are pain, joint movement disorder, local swelling, and sometimes pathological fracture. The vast majority of patients are young people aged 20 to 40 years old, and the average age is about 33 years old [2]. The incidence of giant cell tumor of bone is low, accounting for only about 5% of all primary bone tumors, slightly higher in women than in men [3].

GCTB consists of three types of cells: osteoclast-like multinucleated giant cells, mononuclear oval cells, and mononuclear spindle cells [4]. As the nuclei of oval cells are similar to the nuclei of multinucleated giant cells, many scholars believe that multinucleated giant cells are not tumor cells but stem from mononuclear macrophages [5, 6]. Moreover, some researchers have discovered that GCTB is potentially invasive and has the characteristics of a true tumor after pathological and immunohistochemical assessment, indicating that GCTB is a true neoplasm, as the spindle cells are the proliferating component, but this theory still lacks direct evidence [7-10]. Although the clinical and

https://doi.org/10.62347/BUYC8564

pathological features of GCTB are well known, its nature remains unverified.

The differentiation of a true mesothelial neoplasm from mesothelial hyperplasia can be confirmed by monoclonality, one of the distinguishing characteristics of neoplastic lesions. It is accepted that tumor parenchymal cells are descended from a common progenitor and thus being monoclonal, while reactive lesions are often polyclonal [11, 12]. Clonality analysis based on X chromosome inactivation is a common and classical method to determine the clonality of hyperplasia [11]. According to Lyon's hypothesis, one of the female's two X chromosomes will be permanently inactive due to methylation during embryonic development, inherited from either parent [13-15]. Tumor cells, originating from the same single-cell progenitor, should be monoclonal, and share the same inactivated X chromosome.

Denosumab is a humanized monoclonal antibody that specifically targets Receptor Activator of NF-κB Ligand (RANKL), which is aberrantly expressed and secreted by spindle mononuclear cells. By binding to RANKL and inhibiting the RANKL-RANK axis, denosumab limits the differentiation and maturation of monocyte-macrophages into osteoclasts, reduces bone resorption, and attenuates disease progression [16]. However, denosumab is only used as an adjuvant therapy for unresectable GCTB, or in the case that surgical resection may cause serious complications; while surgical resection is still required for clinical cure. On the other hand, some studies have found that the recurrence rate of GCTB increased after denosumab treatment, reaching 42.8% [17, 18], significantly higher than that of patients without denosumab treatment. Moreover, it has been reported that after denosumab treatment, GCTB has undergone malignant transformation into osteosarcoma, fibrosarcoma and undifferentiated pleomorphic sarcoma [19]. Therefore, it is not clear what function denosumab has on spindle mononuclear cells. Similarly, the therapeutic target against the tumor cells of GCTB is still not clear.

In this study, we aimed to use X chromosome inactivation-based clonality analysis to explore GCTB's clonality and determine whether it is a true neoplasm parenchymal tissue and which cell is the true neoplastic component. Based on established pathology, the neoplastic component of GCTB are stromal-derived spindle cells, which are typically CD68-negative; thus we targeted CD68-negative mononuclear spindle cells for laser capture microdissection (LCM) and clonality analysis. We also aimed to determine the effect of denosumab on tumor cells and seek to find treatment directly targeting true neoplastic cells through drug screening. Hopefully, elucidation of GCTB's nature may provide a novel perspective for its diagnosis and therapy.

Materials and methods

Clinical samples collection

We obtained 32 formalin-fixed paraffin-embedded (FFPE) GCTB tissue blocks from Huashan Hospital of Fudan University (Shanghai, China), along with one FFPE liver cancer sample from a female as a positive control for clonality analysis. For primary cell culture, we also obtained one pair of fresh GCTB surgical samples from a patient before and after denosumab treatment. The patient was a 30-year-old male with GCTB on distal right femur, who was treated at Huashan Hospital. All cases were initially diagnosed by an attending pathologist and reconfirmed by a consulting pathologist. Informed consent was obtained for tissue use in all cases. This study was approved by the Institutional Review Board of School of Basic Medicine, Fudan University (2023-008).

Histologic assessment

Histologic assessment was performed on hematoxylin and eosin (H&E)-stained and immunohistochemistry (IHC) of CD68. GCTB displayed diverse cell types, with multinucleated giant cells, mononuclear oval cells, and mononuclear spindle cells scattered in the focus. Among them, multinucleated giant cells and monocytes were accurately distinguished by H&E staining, while mononuclear spindle cells were identified as CD68-negative and fusiform in shape via IHC.

Immunohistochemistry

Immunohistochemistry for CD68 was performed using a primary antibody (Cat. No.

ab201340; Abcam) at a dilution of 1:100. Briefly, the paraffin embedded tissue was sectioned at 5 μm thickness and placed on slides, dried at 65°C for over 3 hours. After deparaffinization in xylene and alcohol and blocking of endogenous peroxidase in 1% hydrogen peroxide, antigen retrieval was carried out in trypsin (Gibco, Thermo Fisher Scientific, USA) using a 37°C incubator for 1 hour. Sections were blocked with 5% goat serum for 30 minutes, incubated with primary antibody at 4°C overnight, washed with PBS, incubated with secondary antibody (Dako, Agilent) at room temperature for 1 hour, and washed with PBS. Detection was achieved using a standard horseradish peroxidase (HRP)-based detection system (Dako EnVision+ System-HRP, Agilent). Sections were counterstained with hematoxylin. Negative controls were performed by omitting the primary antibody.

Laser capture microdissection (LCM) and genomic DNA extraction

FFPE GCTB tissues, 5 μm thick, were affixed to slides (Applied Biosystems, Foster City, Germany), dried at 65°C for over 3 hours, dewaxed in xylene, and dehydrated with alcohol. Six sections of the same sample were H&E stained, and another six were subjected to CD68 IHC. Multinucleated giant cells, monocytes, and CD68-negative mononuclear spindle cells were accurately captured by laser capture microdissection (LCM) instrument. LCM was performed using an Arcturus XT instrument (Life Technologies). For each cell type, approximately 1,500-3,000 cells were captured per sample. The laser settings were as follows: spot size 7.5-12 μm, power 60-80 mW, duration 8.0-10.0 ms. Captured cells were collected onto CapSure Macro LCM caps (Life technologies).

The genomic DNA of captured cells on the cap was cleaved and extracted as per The PicroPure DNA Extraction Kit (Life Technologies) instructions. Whole tissue DNA was extracted using the QiAamp DNA Micro Kit (Qiagen, Hilden, Germany).

Restriction endonuclease HpaII digestion

The human androgen receptor gene (*HUMARA*) on the X chromosome contains variable CAG short tandem repeats (ranging from 11 to 30), making it a clonality marker. On the inactivated X chromosome, methylation of a CpG site upstream of these repeats prevents *Hpa*II digestion [20], enabling *HUMARA* gene amplification. In heterozygous samples, both of the two homologous X chromosomes may be inactivated. Thus, two fragment sizes are amplified from the genomic DNA of polyclonal non-tumor cells after *Hpa*II digestion. Whereas true tumor cells are monoclonal and exhibit only one fragment size, differing from non-tumor cells. This technique helps identify true tumors [21, 22].

In each case, genomic DNA from LCM-captured multinucleated giant cells, monocytes, and CD68-negative spindle cells was individually assigned to enzyme-digested and undigested subgroups. For the enzyme-digested subgroups, genomic DNA was quantified to 100 ng and subjected to a 3-hour, 37°C digestion using *Hpa*II (New England Biolabs, Beverly, MA). For detailed methods, please refer to our previous research [22].

PCR amplification and data analysis

After *Hpa*II digestion, the reaction mixture was purified using the QIAquick PCR Purification Kit (Qiagen) to remove salts and enzymes. Then, 2 μL purified product was used as template for PCR amplification. *HUMARA* gene amplification was performed using nested PCR. The outer primers were: 5'-TCC AGA ATC TGT TCC AGA GCG TGC-3' and 5'-GCT GTG AAG GTT GCT GTT CCT CAT-3'. The inner primers (fluorescently labeled with 6-FAM) were: 5'-GCA GCG CTC CGA GAA GTT CCT GTT C-3' and 5'-GCT GGG AAC GGG GCT CCC CAG AAC-3'. The PCR reaction mixture (25 μL) contained 1× PCR buffer, 200 μM dNTPs, 0.2 μM of each primer, 1 U of Taq DNA polymerase (TaKaRa), and 2 μL of template DNA. Initial denaturation was performed at 95°C for 10 minutes, followed by 34 cycles of 30 seconds at 94°C, 30 seconds at 64°C, and 30 seconds at 72°C, with final extension at 72°C for 10 minutes.

The fluorescence intensity detected by capillary electrophoresis appears as a peak map. In theory, *Hpa*II-undigested *HUMARA* DNA from heterozygote yields two peaks: Allele 1 and Allele 2. A set of tightly clustered multiple peaks was adjacent to the major product peak due to Taq polymerase slippage during amplification [12,

Table 1. The sequences of primers in RT-qPCR

Primer	Sequence 5'-3'
GAPDH_F	CTGACTTCAACAGCGACACC
GAPDH_R	TGCTGTAGCCAAATTCGTTGT
PDGFRA_F	TGGCAGTACCCCATGTCTGAA
PDGFRA_R	CCAAGACCGTCACAAAAAGGC
PDGFRB_F	AGACACGGGAGAATACTTTTGC
PDGFRB_R	AGTTCCTCGGCATCATTAGGG
PDGFD_F	TTGTACCGAAGAGATGAGACCA
PDGFD_R	GCTGTATCCGTGTATTCTCCTGA
RUNX2_F	TGGTTACTGTCATGGCGGGTA
RUNX2_R	TCTCAGATCGTTGAACCTTGCTA
BCL2_F	GGTGGGGTCATGTGTGTGG
BCL2_R	CGGTTCAGGTACTCAGTCATCC
MCL1_F	GTGCCTTTGTGGCTAAACACT
MCL1_R	AGTCCCGTTTTGTCCTTACGA
BCL2L1_F	GAGCTGGTGGTTGACTTTCTC
BCL2L1_R	TCCATCTCCGATTCAGTCCCT
RBL2_F	TGAGCGAAAGCTACACGCTG
RBL2_R	TCCCTTTGCTTACAGTTGGAAC

22]. Obvious peaks were thus selected as main peaks for clonality analysis. To account for the preferential amplification of non-specific short fragments that could affect *HUMARA* gene amplification, we calculated the corrected cleavage ratio. It's defined as:

$$\text{Cleavage Ratio} = \frac{\text{area of the main peak at Allele 1 before digestion/area of the main peak at Allele 1 after digestion}}{\text{area of the main peak at Allele 2 before digestion/area of the main peak at Allele 2 after digestion}}$$

Samples with cleavage ratio above 2.0 or below 0.5 were considered to be monoclonal tumor tissues [23], and the corresponding cells were identified as tumor cells.

Isolation of GCTB primary cells

The isolation of GCTB primary cells was carried out as previously described [24-26]. Briefly, fresh surgical samples of GCTB were cut into small tissue blocks of approximately 1 mm^3 in size and washed with PBS. The tissue blocks were digested by 0.2% type II collagenase (Thermo Fisher Scientific, USA)-DMEM medium in a constant temperature incubator at 37°C overnight. The digest was filtered through a 70 μm cell screen and centrifuged at 1,500 rpm for 5 min. The supernatant was discarded, and the deposition was resuspended in 10% FBS-DMEM culture medium, and seeded into dishes.

CCK-8 assay

The cells were seeded at a density of 8,000 cells/well in a 96-well plate. For denosumab (Xgeva, Amgen, USA), cells were treated with concentrations ranging from 10 to 800 μg/mL for 48 h, and concentration of 800 μg/mL from 24 to 120 h. For Avapritinib (Selleckchem, USA) and Capivasertib (Selleckchem), cells were treated with concentrations ranging from 0.1 to 100 μM for 48 h. Control groups received an equal volume of vehicle (PBS for denosumab, DMSO for inhibitors, with final DMSO concentration <0.1%). After adding the CCK-8 reagent (Yeasen, Shanghai, China), the plate was incubated at 37°C for 2 h. The optical density (OD) value was measured at 450 nm wave length by Multiskan GO spectrophotometer (Thermo Fisher Scientific).

RT-qPCR

Total RNA was isolated with FreeZol Reagent (Vazyme, Nanjing, China) from cells. cDNA was reverse transcribed with HiScript IV RT SuperMix (Vazyme). The Real-time quantitative PCR reaction system (20 μL) contained 1× ChamQ Universal SYBR qPCR Master Mix (Vazyme), 0.4 μM each primer, and 1 μL of cDNA template. The expression level of PDGFRA, PDGFRB, PDGFD and RUNX2 RNA were normalized by GAPDH. The sequences of primers (Sangon Biotech, Shanghai, China) are shown in **Table 1**. The detection was carried out using a LightCycler 480 (Roche, Switzerland). The reaction conditions included an initial denaturation step at 95°C for 30 s, followed by 40 cycles of denaturation at 95°C for 10 s and annealing/extension at 60°C for 30 s. The relative expression levels were calculated using the $2^{-\Delta\Delta Ct}$ method.

Statistical analysis

All data are presented as mean ± SEM. Statistical analysis was performed with unpaired two-tailed Student's t test, or one-way or two-way analysis of variance (ANOVA) followed by Bonferroni's posttest, in GraphPad Prism 5.0. *p*-value <0.05 was considered to be statistically significant.

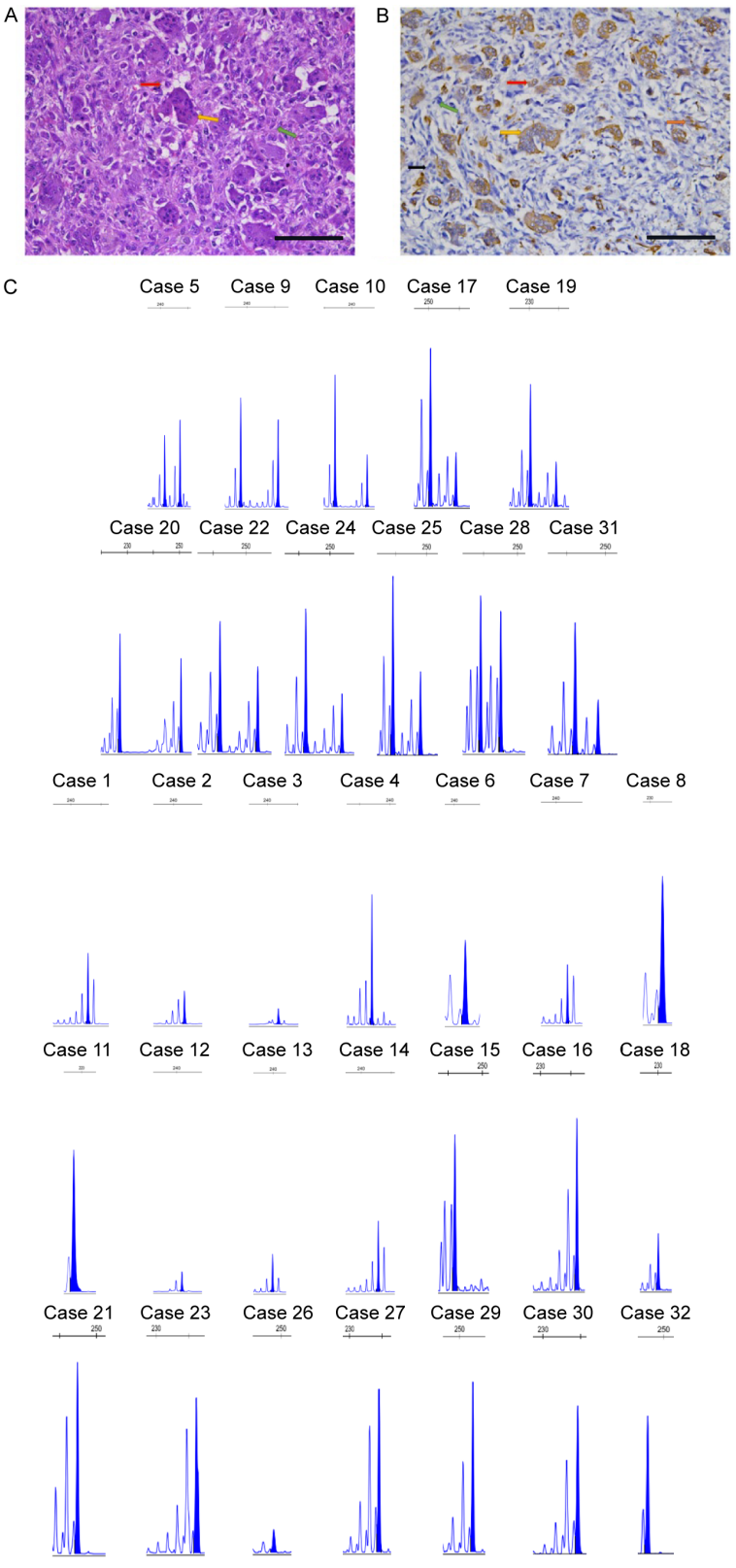

Figure 1. Typical pathological morphology, IHC detection of CD68, and *HUMARA* polymorphism of GCTB. A. Multinucleated giant cells (yellow arrow), mononuclear oval cells (red arrows), and mononuclear spindle cells (green arrow) were able to be detected by H&E stained (×200). B. Yellow arrow: multinucleated giant cells with CD68-positive; red arrows: CD68-positive mononuclear oval cells; green arrow: CD68-negative mononuclear spindle cells; black arrow: CD68-negative mononuclear oval cells; orange arrow: CD68-positive mononuclear spindle cells (×200). C. The *HUMARA* locus was heterozygous in 11 cases: No. 5, 9-10, 17, 19, 20, 22, 24-25, 28, and 31, while they were homozygous in the other cases. Scale bar 100 μm. *HUMARA*: human androgen receptor gene; GCTB: giant cell tumor of bone.

Results

Morphological characteristic of GCTB

Typical GCTB tissue was basically composed of three types of cells: multinucleated giant cells, mononuclear oval cells, and mononuclear spindle cells (**Figure 1A**). Multinucleated giant cells were scattered among mononuclear cells in large numbers, with many nuclei. IHC staining showed that multinucleated giant cells and part of the mononuclear oval cells were CD68-positive, while another part of mononuclear oval cells and mononuclear spindle cells were negative (**Figure 1B**). The CD68-negative mononuclear spindle cells, which were the focus of our clonality analysis, exhibited elongated, fusiform shapes with scant cytoplasm and oval nuclei, distinct from the rounder CD68-positive mononuclear cells.

Prior to clonality analysis, the polymorphism of the samples' *HUMARA* gene must be confirmed. DNA was extracted from 32 GCTB cases. The *HUMARA* gene was amplified, and the gene polymorphism was detected (**Figure 1C**; **Table 2**). Eleven of 32 cases were *HU-*

Table 2. Clinical features and *HUMARA* polymorphisms of the 32 GCTB patients

Case no.	Age (y)	Site	*HUMARA*	Case no.	Age (y)	Site	*HUMARA*
1	55	NA	Homozygous	17	21	the head and neck of right femur	Heterozygous
2	28	the left radius	Homozygous	18	26	the distal part of the left femur	Homozygous
3	64	the left tibia	Homozygous	19	40	the proximal part of the left tibia	Heterozygous
4	33	the lower end of the left femur	Homozygous	20	22	the distal part of the left femur	Heterozygous
5	62	the lower end of the left femur	Heterozygous	21	29	the proximal part of the left tibia	Homozygous
6	37	the sacral region	Homozygous	22	23	the left femur	Heterozygous
7	50	the lower end of the left femur	Homozygous	23	48	the distal part of the left femur	Homozygous
8	22	the right tibia	Homozygous	24	52	the proximal part of the left tibia	Heterozygous
9	60	the distal part of the left femur	Heterozygous	25	25	the proximal part of the right femur	Heterozygous
10	27	the region of bone saddle	Heterozygous	26	27	the proximal part of the left tibia	Homozygous
11	23	the proximal part of the tibia	Homozygous	27	15	the proximal part of the right tibia	Homozygous
12	39	the right wrist	Homozygous	28	22	the parahumeral soft tissue of right upper arm	Heterozygous
13	40	the right radius	Homozygous	29	31	the distal part of the left femur	Homozygous
14	42	the right acromion	Homozygous	30	15	the proximal part of the left femur	Homozygous
15	26	the distal part of the left femur	Homozygous	31	32	the distal part of the right femur	Heterozygous
16	57	the proximal part of the right tibia	Homozygous	32	25	the proximal part of the left humerus	Homozygous

NA: not available; *HUMARA*: human androgen receptor gene; GCTB: giant cell tumor of bone.

MARA-heterozygous, which were suitable for further analysis.

The multinucleated giant cells in GCTB are polyclonal hyperplasia

As there are mainly three types of cells in GCTB, clonality analysis was performed on each type to confirm the genuine neoplastic cell population within this tumor.

Before analyzing GCTB, in order to ensure the methodological feasibility and result reliability, hepatoma cells were selected as a positive control. The hepatoma cells showed 1 peak through digestion with *Hpa*II, indicating that the cells were monoclonal, while liver cancer was a neoplastic hyperplasia (**Figure 2A**).

We chose to analyze the clonality of the osteoclastic multinucleated giant cells first. The multinucleated giant cells were captured by LCM machine (**Figure 2B**). The DNA of captured multinucleated giant cells was extracted, digested and non-digested, and amplified by *HUMARA* primer with 6-FAM fluorescence. The PCR products were subjected to capillary electrophoresis, and the fluorescence intensity peak map was analyzed.

The results showed that the two representative cases (No.10 and 25) were both polyclonal (**Figure 2C**), which indicated that osteoclast-like multinucleated giant cells were polyclonal hyperplasia, and were not the neoplastic component of GCTB. Analysis of multinucleated giant cells from all 11 informative (heterozy-

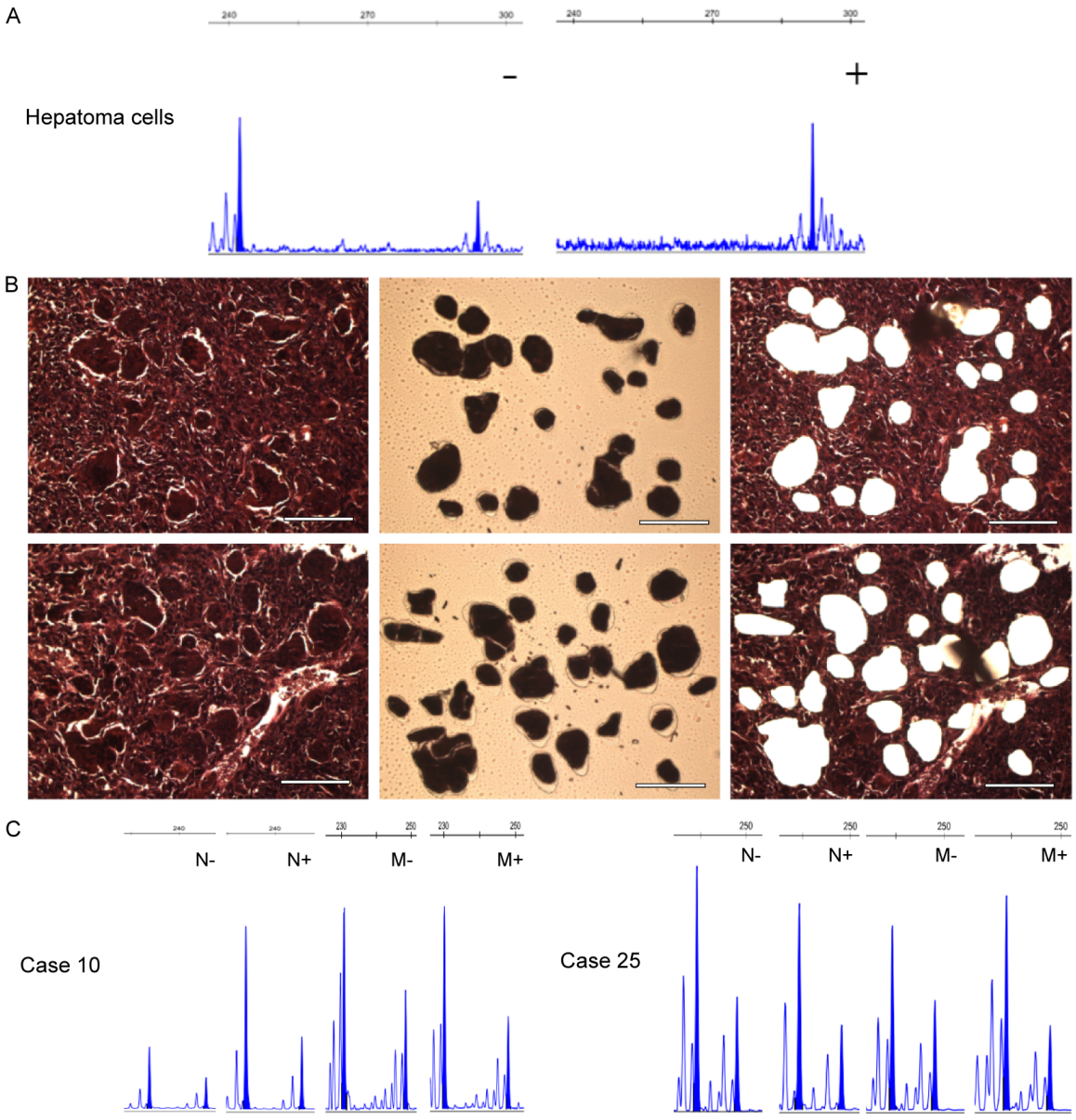

Figure 2. *HUMARA* polymorphism of hepatocellular carcinoma and multinucleated giant cells in GCTB. A. *HUMARA* polymorphism of hepatoma cells. B. LCM captured multinucleated giant cells in GCTB in Case No. 10 and 25 (×400). C. HUMARA polymorphism in Case No. 10 and 25. N, normal tissue of GCTB; M, LCM-captured multinucleated giant cells; -, non-digestion with *Hpa*II; +, digestion with *Hpa*II. Scale bar 50 μm. LCM: laser capture microdissection.

gous) cases revealed polyclonal patterns, consistent with reactive hyperplasia (Supplementary Table 1).

The mononuclear spindle cells in GCTB are the true tumor components of GCTB

We further accurately captured mononuclear cells around multinucleated giant cells to explore their clonality. The results showed that the mononuclear cells were polyclonal in most cases, while monoclonal in very few cases. **Figure 3** demonstrated the results that the two cases (No. 10 and 25) were still polyclonal. Since mononuclear cells can be divided into two kinds: oval cells and spindle cells, we believed this needed further classification, as one of them could be the true neoplastic component.

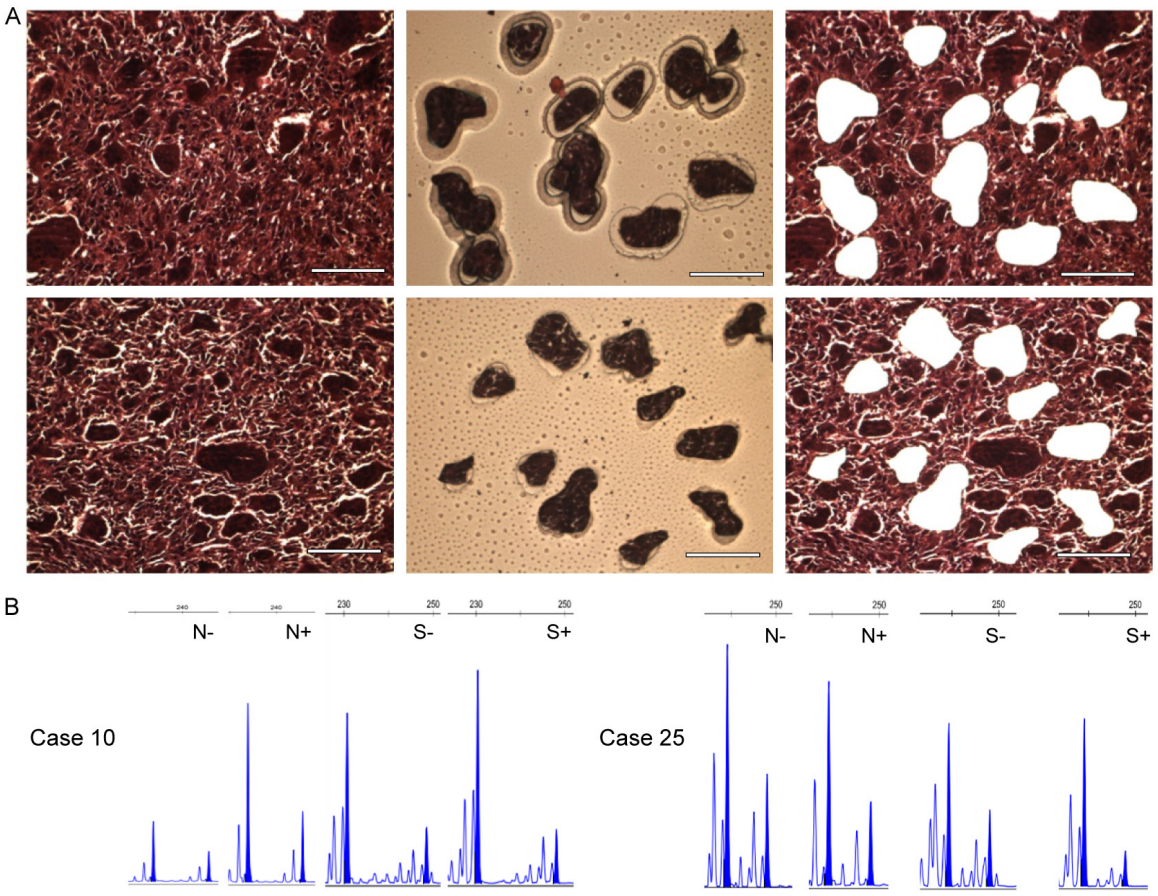

Figure 3. *HUMARA* polymorphism of Mononuclear cells in GCTB. A. LCM captured mononuclear cells in GCTB in Case No. 10 and 25 (×400). B. *HUMARA* polymorphism in Case No. 10 and 25. N, normal tissue of GCTB; S, LCM-captured mononuclear cells; -, non-digestion with *Hpa*II; +, digestion with *Hpa*II) Scale bar 50 μm.

Based on the established pathological concept that the neoplastic component in GCTB is the stromal-derived spindle cell, which are typically CD68-negative, we targeted CD68-negative mononuclear spindle cells for LCM and clonality analysis. We used LCM to capture CD68-negative mononuclear spindle cells and extract their DNA for clonality analysis (**Figure 4A**). In 2 representative cases, No. 10 and 25, there was only one peak after digestion with *Hpa*II enzyme (**Figure 4B**). Analysis of CD68-negative spindle cells from all 11 informative (heterozygous) cases showed a monoclonal pattern (Supplementary Table 1). Monoclonality, as determined by X-inactivation analysis, is a well-established hallmark of neoplastic proliferation, indicating origin from a single progenitor cell. The results showed that CD68-negative mononuclear spindle cells were monoclonal and were true neoplastic cells of GCTB, which further demonstrated that GCTB was a true tumor.

Isolation and identification of GCTB primary tumor cells

Primary cell isolation was performed on fresh tumor tissue from a patient with GCTB before and after denosumab treatment. One day after isolation and culture, three main types of cells in GCTB were observed: mononuclear spindle cells, mononuclear round cells, and multinucleated giant cells (**Figure 5A**). After 2-3 passages, the only remaining primary cells were mononuclear spindle-shaped cells, while multinucleated giant cells and other cells disappeared (**Figure 5B**). The passaged primary cells were used for further study.

To identify the isolated primary cells, cellular immunofluorescence staining was performed. Immunofluorescence staining showed that mutant histone H3.3 (G34W) was strongly positive in the nucleus in approximately 90% of the iso-

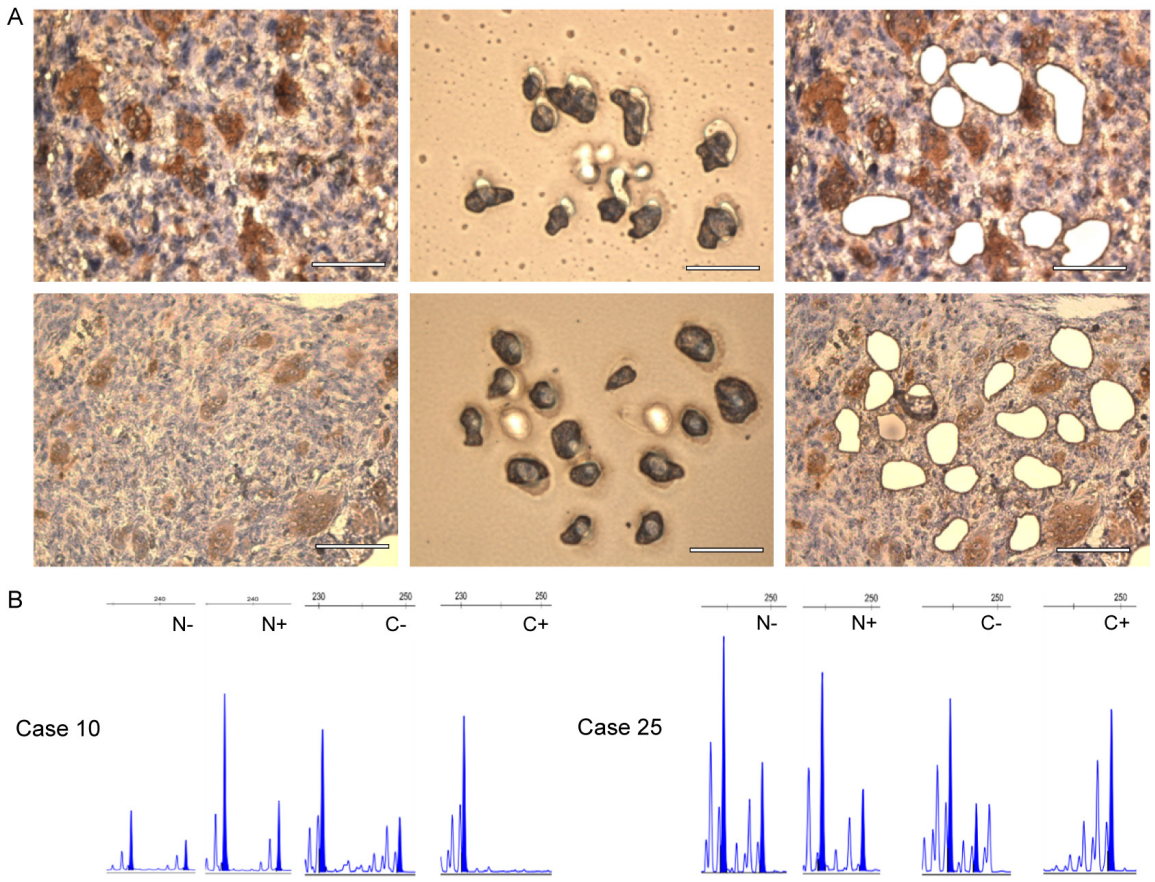

Figure 4. *HUMARA* polymorphism of CD68-negative mononuclear spindle cells in GCTB. A. LCM captured mononuclear cells in GCTB in Case No. 10 and 25 (×400). B. *HUMARA* polymorphism in Case No. 10 and 25. N, normal tissue of GCTB; C, LCM-captured CD68-negative mononuclear spindle cells; -, non-digestion with *Hpa*II; +, digestion with *Hpa*II. Scale bar 50 μm.

lated adherent spindle cells, while CD68 was negative. (**Figure 5C**). Negative controls, performed by omitting the primary antibody, showed no signal. A known GCTB tissue section served as the positive control for the antibody. For further confirmation, DNA was extracted from primary cells and PCR amplification and Sanger sequencing were performed on the fragment near H3-3A G34W. Sequencing revealed a mutation at H3-3A G34W site in primary cells (**Figure 5D**). These results proved that the isolated primary cells were the tumor cells of giant cell tumor of bone.

Denosumab has no direct effect on the growth of GCTB tumor cells but indirectly changes the phenotype of GCTB tumor cells

Denosumab has a certain clinical effect on GCTB that makes it difficult to resect or it can cause serious complications after resection. However, the optimal administration time and dosing of denosumab are still not completely unified [16].

A high concentration (800 μg/mL) was included based on some in vitro studies [27, 28], although it exceeds typical serum levels. The primary tumor cells were treated with denosumab from 10 to 800 μg/mL for 48 h. Compared with the control group, different concentrations of denosumab had no direct effect on cell growth (**Figure 5E**). The tumor cells were treated with 800 μg/mL denosumab continuously. The growth of cells at 24 h, 48 h, 72 h, 96 h and 120 h did not change compared with the control group (**Figure 5F**).

We inquired whether denosumab could change the phenotype of GCTB tumor cells. RUNX family transcription factor 2 (RUNX2) is essential for osteoblastic differentiation and skeletal

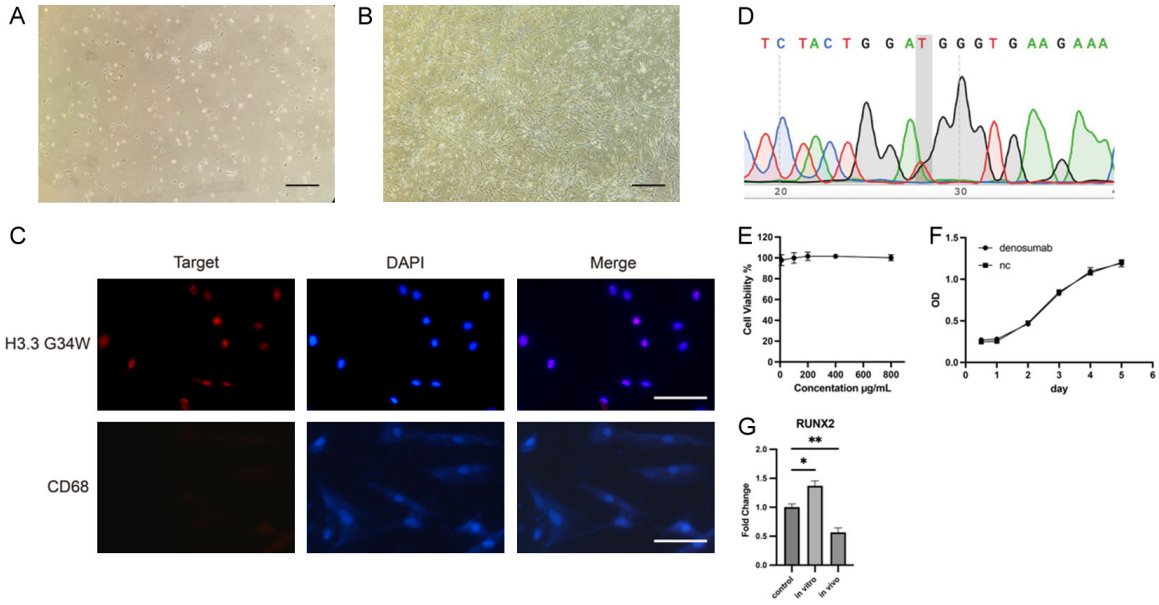

Figure 5. The effect of denosumab on GCTB primary tumor cells. A, B. The isolated primary cells from GCTB after 1 day and 2-3 passages (×40, Scale bar 100 μm). C. The primary cells were positive for H3.3 G34W in nucleus and negative for CD68 (×400, Scale bar 50 μm). D. Sanger sequencing showed the primary cells exhibited a mutation at the H3-3A G34W site. E. Different concentrations of denosumab had no direct effect on the primary tumor cells' growth. F. 800 μg/mL denosumab had no direct effect on the primary tumor cells' growth in 120 h. G. RUNX2 RNA increased after denosumab treatment *in vitro*, but decreased after treatment *in vivo*. *, $P<0.05$; **, $P<0.01$. RUNX2: RUNX family transcription factor 2.

morphogenesis and acts as a scaffold for nucleic acids and regulatory factors involved in skeletal gene expression [29]. qPCR showed that RUNX2 RNA increased after denosumab treatment *in vitro* ($P<0.05$), but decreased after treatment *in vivo* ($P<0.01$, **Figure 5G**). These results indicate that denosumab, at the tested concentrations, has no direct anti-proliferative effect on cultured GCTB tumor cells *in vitro*. The opposite changes in RUNX2 RNA expression observed *in vitro* versus *in vivo* samples suggest that the drug's effects on tumor cell phenotype may be context-dependent, potentially involving the bone microenvironment.

PDGFRAi has a direct effect on the growth of GCTB tumor cells and changes the phenotype of GCTB tumor cells

Platelet derived growth factor receptor alpha (PDGFRA), a member of receptor tyrosine kinase family, plays an important role in embryonic development, cell proliferation, survival and chemotaxis [30]. Avapritinib is a potent and selective inhibitor of PDGFRA (PDGFRAi) and KIT kinases. In addition to inhibiting the activation loop of wild-type PDGFRA and KIT kinases, it also has potent inhibition of PDGFRA D824V and KIT D816V mutants. High-throughput drug screening showed that Avapritinib at 3 μM concentration had no significant inhibitory effect on other kinases [31].

Primary tumor cells were treated with Avapritinib (0.1-100 uM) for 48 h. Avapritinib inhibited tumor cell growth in a dose-dependent manner, as the cell viability decreased to 50.54% with the concentration of 100 μM (**Figure 6A**).

Subsequently, we treated primary tumor cells with 10 μM Avapritinib for 24 h and detected the expression of related genes. Avapritinib upregulated the mRNA expression of PDGFRA ($P<0.001$), PDGFRB ($P<0.05$), PDGFD ($P<0.01$) and RUNX2 ($P<0.05$) in primary tumor cells (**Figure 6B**). These findings indicate that PDGFRAi could inhibit the growth of primary tumor cells and alter the phenotype of primary tumor cells.

PDGFRAi regulates the growth and phenotype of GCTB tumor cells through the PI3K/AKT pathway

The PI3K/AKT/mTOR pathway plays a key role in the occurrence and development of many

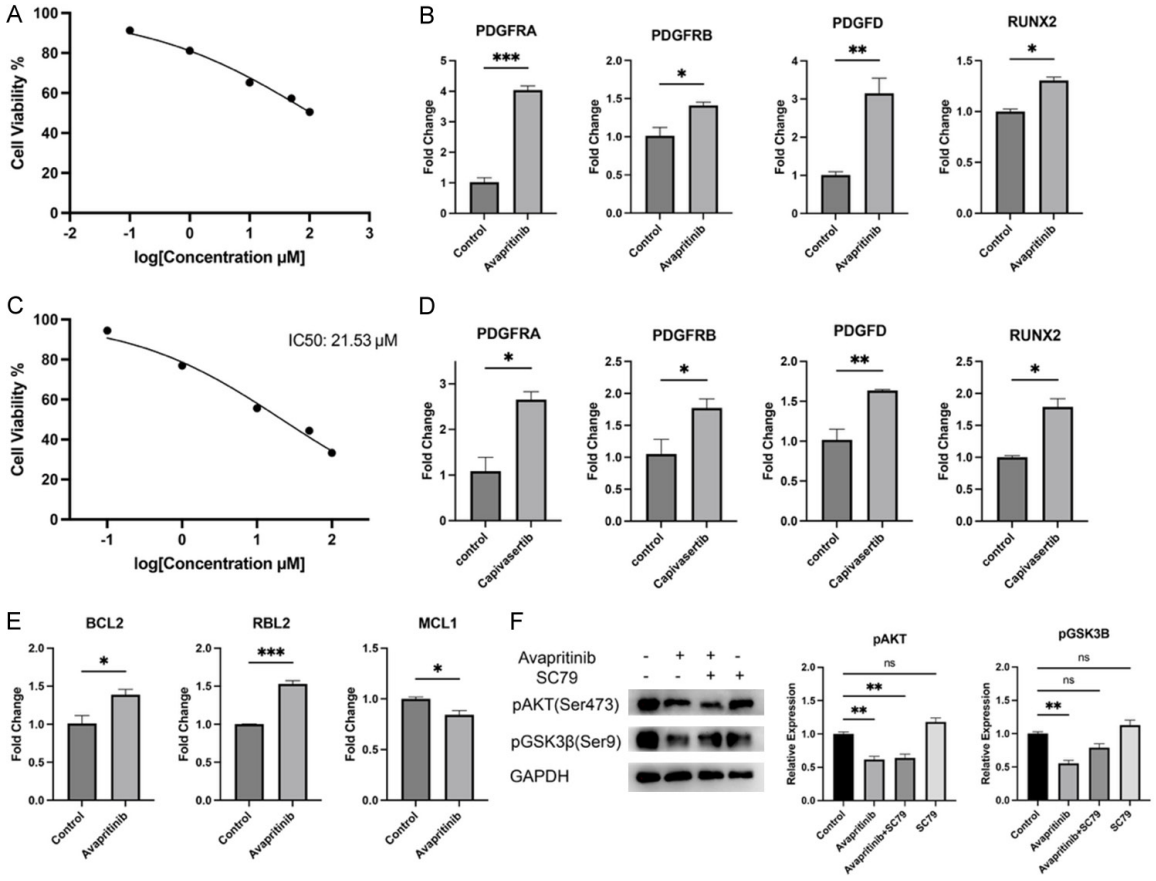

Figure 6. PDGFRAi can regulate the growth and phenotype of GCTB tumor cells through the PI3K/AKT pathway. A. Avapritinib inhibited tumor cell growth in a dose-dependent manner. B. Avapritinib up-regulated the mRNA level of PDGFRA, PDGFRB, PDGFD and RUNX2 in primary tumor cells. C. Capivasertib inhibited the growth of tumor cells in a dose-dependent manner. The IC50 of Capivasertib on tumor cell growth was 21.53 μM. D. Capivasertib up-regulated PDGFRA, PDGFRB, PDGFD and RUNX2 RNA in tumor cells. E. Avapritinib had an effect on AKT-related genes in tumor cells, up-regulating BCL2 and RBL2 RNA, and down-regulating MCL1 RNA. F. Avapritinib down-regulated pAKT and pGSK3β, which was partly reversed by SC79. Ns, no significance; *, $P<0.05$; **, $P<0.01$; ***, $P<0.001$. PDGFRAi: PDGFRA inhibitor; PDGFRA: platelet derived growth factor receptor alpha; PDGFRB: platelet derived growth factor receptor beta; PDGFD: platelet derived growth factor D; BCL2: B-cell lymphoma 2 apoptosis regulator; RBL2: RB transcriptional corepressor like 2; MCL1: Myeloid cell leukemia 1 apoptosis regulator; pGSK3β: phosphorylated GSK3β (Ser9).

kinds of tumors, regulating cell proliferation, apoptosis and metabolism. There are three isoforms of PI3K: I, II and III. Type I PI3K is a heterodimeric structure composed of a catalytic subunit and a regulatory subunit, which can be further subdivided into types IA and IB. The former is activated by receptor tyrosine kinases (RTKs) and the latter by G protein-coupled receptors (GPCRs). PDGFRA is a member of the RTK family. When the ligand specifically binds to it, signal transduction adaptor proteins are phosphorylated, thereby activating type IA PI3K and activating downstream pathways [32].

Capivasertib is an orally active, broad-spectrum AKT inhibitor with inhibitory activity against AKT1, AKT2, and AKT3. Capivasertib has anti-tumor activity and can be used to treat breast cancer, and it is currently in phase I clinical trials.

Primary tumor cells were treated with Capivasertib (0.1-100 μM) for 48 h. Capivasertib inhibited the growth of tumor cells in a dose-dependent manner, and the IC50 of Capivasertib on tumor cell growth was 21.53 μM (**Figure 6C**).

Subsequently, we treated the primary tumor cells with 10 μM Capivasertib for 24 h and detected the expression of related genes. Capivasertib up-regulated the mRNA level of

PDGFRA ($P<0.05$), PDGFRB ($P<0.05$), PDGFD ($P<0.01$) and RUNX2 ($P<0.05$) in tumor cells (**Figure 6D**). AKT inhibitor can inhibit the growth of GCTB cells and change the cell phenotype, which is consistent with the effect of PDGFRAi. Moreover, Avapritinib modulated the expression of AKT-related genes in tumor cells, up-regulating the mRNA level of B-cell lymphoma 2 apoptosis regulator (BCL2, $P<0.05$) and RB transcriptional corepressor like 2 (RBL2, $P<0.001$), and down-regulating the mRNA level of Myeloid cell leukemia 1 apoptosis regulator (MCL1, $P<0.05$, **Figure 6E**).

Western blot analysis showed that treatment with 5 μM Avapritinib for 24 h decreased the levels of phosphorylated AKT (Ser473, p-AKT, $P<0.01$) and its downstream target phosphorylated GSK3β (Ser9, pGSK3β, $P<0.01$) in primary tumor cells. Co-treatment with the AKT agonist SC79 (10 μM) partially restored the levels of pAKT and pGSK3β (**Figure 6F**). These finding indicate that PDGFRAi regulates the growth and phenotype of GCTB tumor cells through the PI3K/AKT pathway.

Discussion

GCTB is classified by the WHO as an intermediate tumor with a high recurrence rate and potential malignancy, accounting for about 5% of benign bone tumors [2]. Miller et al. found that GCTB can metastasize in the lung [33]. Quatma et al. also reported a case that can be transformed into epithelioid angiosarcoma [34]. In addition, Fumiaki Masul et al. believed that mononuclear stromal cells and osteoclast-like multinucleated giant cells were induced by a variety of cytokines, which were induced in an autocrine or paracrine manner, and that was closely related to the invasiveness of GCTB [35]. Above all, GCTB exhibits the characteristics of true neoplasm parenchymal. Before our research, a clonality analysis of giant cell tumors by Schwartz et al. detected all specimens were polyclonal indicating that GCTB was a non-neoplastic proliferation of mesenchymal cells [36]. However, the cell composition of GCTB is complex, and its cell component has three types: multinucleated giant cells, mononuclear oval cells, and mononuclear spindle cells [37]. Our study performed a more accurate clonality analysis based on cellular components and confirmed that GCTB is a true tumor, and CD68-negative mononuclear spindle cells are its tumor cells.

Multinucleated giant cells in GCTB were polyclonal, indicating that they were reactive hyperplasia cells rather than neoplasm cells. In this study, laser capture microdissection was used to accurately separate and harvest multinucleated giant cells in GCTB. The results of clonality analysis indicated that it was a polyclonal origin, which proved that it is a non-tumor component. GCTB is named for its abundant multinucleated giant cells, whereas our results suggested that multinucleated giant cells are not neoplasm cells. Therefore, it is not appropriate to classify GCTB as osteoclasts.

The mononuclear cell components of GCTB are complex, which can't be distinguished by H&E staining. It is well known that CD68 is a marker for monocyte-macrophage cell lines [38]. Previous researchers found that CD68 was strongly positive in osteoclast-like multinucleated giant cells and mononuclear oval cells, and generally negative in mononuclear spindle cells with occasionally positive expression [9, 39, 40]. Our study differentiated mononuclear cells by immunological expression of CD68 and discovered that the clonality of CD68-negative spindle cells in mononuclear cells was inconsistent with the whole monocytes. CD68-negative mononuclear cells are monoclonal proliferative tumor cells, most of which are mononuclear spindle cells. The CD68-positive cells, including multinucleated giant cells and some of the mononuclear cells, are polyclonal hyperplasia, which is similar to the reactive hyperplasia of granuloma. This phenomenon further explains why previous studies had found heterogeneity in the expression of CD68 in GCTB.

Only the CD68-negative mononuclear spindle cells are the genuine tumor cells in GCTB, not all the mononuclear cells. In previous publications, mononuclear stromal cells were thought to be the true neoplastic components of GCTB. However, their results are only presented in the form of immunohistochemistry and cannot be used as favorable evidence [41]. Some scholars have also suggested this assumption based on these cells have strong growth and proliferation abilities both in vivo and in vitro [42]. In this study, we identified CD68-negative mononuclear cells as monoclonal hyperplasia using clonal-

ity analysis based on X chromosome inactivation, strongly suggesting that they are true tumor components of GCTB.

During primary cell isolation, overnight digestion was performed with type II collagenase according to published literature [24-26]. It is known that the primary cells have the characteristics of fragility and significant batch-to-batch variations. Our primary cells showed a good viability in morphology on the day after isolation and the CCK8 assay after enrichment and passage, which were suitable for subsequent functional experiments. Nonetheless, it is reported that type I collagenase has relative average activity of multiple enzymes [43], shortening the digestion duration while better preserving cell viability. Combined usage of type I and type II collagenases may lead to a higher digestion efficiency [44], representing a promising optimization strategy for future primary cell preparation.

H3.3 G34W is a mutant histone protein, which is manifested as a mutation from glycine (G) to tryptophan (W) in the 34th amino acid of histone H3.3 [45]. This mutation is common in giant cell tumor of bone, which is the key mutation to maintain the poor differentiation and abnormal proliferation of tumor cells, and is often used to assist in the diagnosis of giant cell tumor of bone clinically [46]. Immunofluorescence staining revealed strong nuclear positivity for H3.3 G34W in approximately 90% of the isolated adherent spindle cells, indicating that the most primary cells used in our subsequent experiments were tumor cells from giant cell tumor of bone. In the future, the direct clonality analysis of the H3.3 G34W-positive cells in GCTB needs to be performed to strengthen our findings.

Denosumab, as a neoadjuvant therapy, provides new possibilities for treating GCTB. However, the effect of denosumab on CD68-negative spindle tumor cells remains unknown [16]. We treated primary tumor cells with denosumab in vitro. Our findings suggest that denosumab inhibits the formation of osteoclastic multinucleated giant cells but has no direct effect on the growth of spindle mononuclear tumor cells. As C. P. Lau et al. [47] also found that the proliferation of GCTB tumor cells was not inhibited by denosumab therapy. However, MAK I W et al. [48] collected six samples of giant cell tumor of bone, two of which were treated with denosumab, and subjected to primary cell isolation and culture. It was found that after denosumab treatment, tumor cells were still present, but their growth rate in vitro was reduced by about 50%. We believe that the difference in tumor growth rate in this study may be due to the changes in tumor microenvironment caused by in vivo denosumab treatment and cell-to-cell interactions, or the tumor heterogeneity among patient samples.

It is found that denosumab induced opposite changes in RUNX2 RNA expression *in vitro* versus *in vivo* samples. A. Schubert et al. [28] treated osteoblastic lineage cells from the alveolar bone with denosumab *in vitro*, and found that denosumab increased RUNX2, which is the same as our finding, while reduced the level of collagen I, and had no significant change in RANKL. X. Chen et al. [27] found that p62 was down-regulated after denosumab treatment *in vivo*, but the effect cannot be reproduced *in vitro*. All these findings suggested that the drug's effects on tumor cell phenotype may be context-dependent.

PDGFRA, a member of RTK family, is an important factor in bone development and skull closure during embryonic development, and also plays a role in mesenchymal stem cell recruitment and intestinal villus development during gastrointestinal mucosal development. PDGFRA has shown significant potential as a therapeutic biomarker in various tumors, such as gastrointestinal stromal tumor (GIST) [49], pediatric high-grade glioma (pHGC) [50] and others.

We hypothesized that PDGFRA may play an important role in GCTB tumor cell growth. We found that the growth of tumor cells was inhibited by Avapritinib. Meanwhile, the mRNA expression of PDGFRA, PDGFRB, PDGFD, and RUNX2 was up-regulated by Avapritinib in tumor cells. Previous studies have found that the RTKs in GCTB are highly phosphorylated, including EGFR, Axl, RYK, PDGFRB, ALK, and IGF-IR. Sunitinib, an inhibitor of PDGFRB, can inhibit the growth of bone giant cell tumor cells. Denosumab combined with Sunitinib can successfully inhibit the growth of osteoclastic multinucleated giant cells and spindle mononuclear cells in tumor tissues of patients [51]. However, the downstream pathway of PDGFRB

has not been further explored. PDGFRA and PDGFRB belong to the platelet-derived growth factor receptor family in the RTK family and have similarities in structure and function. Our finding showed that PDGFRA inhibitor also inhibited the growth of GCTB tumor cells.

It has been reported that the PI3K/AKT/mTOR pathway plays a key role in the occurrence and development of a variety of tumors, regulating cell proliferation, apoptosis and metabolism [52]. However, PI3K can be activated by RTKs and activate the downstream AKT pathway [32, 53]. *In vitro* treatment of primary tumor cells showed that AKT inhibitor Capivasertib had a dose-dependent inhibitory effect on tumor cell growth with an IC50 of 21.53 μM. Meanwhile, Capivasertib treatment could up-regulate the mRNA expression of PDGFRA, PDGFRB, PDGFD, and RUNX2 in tumor cells, which was consistent with the effect of PDGFRAi. pGSK3β, an important downstream of PI3K/AKT pathway, was down-regulated by Avapritinib treatment, and partly reversed by co-treatment with AKT agonist. Therefore, we suggested that PI3K/AKT is one of the downstream pathways of PDGFRA.

This study has several limitations. First, the clonality analysis was based on X-inactivation and is therefore applicable only to female patients, limiting the sample size for informative cases. Second, the primary cell culture, despite our enrichment steps, may still contain a small fraction of non-neoplastic cells, which could influence drug response assays. Third, although the viability of the primary cells after enrichment and passage was acceptable for subsequent experiments, the primary cells have the characteristics of fragility and significant batch-to-batch variations, which may affect the reproducibility of experiments. It is recommended to conduct cell counting and cell viability assays immediately after primary cell isolation to obtain the baseline data for the primary cells, which will facilitate comparisons between different batches. Fourth, our functional studies on PDGFRA/PI3K/AKT signaling were performed mainly in vitro using cells from a limited number of patients. Future studies with larger cohorts, in vivo models, and investigations into the interplay between neoplastic spindle cells and other cellular components in the GCTB microenvironment are warranted to fully validate these findings and explore therapeutic potential.

Our findings will be helpful for understanding the nature of GCTB and pioneering novel targeted therapies. Although the mystery of GCTB is gradually uncovered by scholars, many unresolved questions remain, including the interactions among components of GCTB, its pathogenesis and underlying mechanisms, as well as the disease-related signaling pathways.

Conclusion

GCTB is a true neoplasm, with CD68-negative mononuclear spindle cells identified as the monoclonal neoplastic component. PDGFRA inhibition directly suppresses the growth of these tumor cells and alters their phenotype, likely through modulation of the PI3K/AKT signaling pathway. These findings suggest PDGFRA as a potential novel therapeutic target for GCTB, warranting further investigation.

Acknowledgements

We acknowledge Michael Cao (Shanghai Medical College of Fudan University) for the linguistic editing and proofreading during the preparation of this manuscript.

Disclosure of conflict of interest

None.

Address correspondence to: Dr. Shuyang Wang and Hongguang Zhu, Department of Pathology, School of Basic Medicine, Fudan University, No. 131 Dong'an Road, Xuhui District, Shanghai, China. E-mail: shuyangwang@fudan.edu.cn (SYW); hongguang_702@163.com (HGZ)

References

[1] Aoude A, Nikomarov D, Perera JR, Ibe IK, Griffin AM, Tsoi KM, Ferguson PC and Wunder JS. Giant cell tumour of bone. Bone Joint J 2023; 105-B: 559-567.

[2] Balke M, Schremper L, Gebert C, Ahrens H, Streitbuerger A, Koehler G, Hardes J and Gosheger G. Giant cell tumor of bone: treatment and outcome of 214 cases. J Cancer Res Clin Oncol 2008; 134: 969-978.

[3] Basu Mallick A and Chawla SP. Giant cell tumor of bone: an update. Curr Oncol Rep 2021; 23: 51.

[4] Jha Y and Chaudhary K. Giant cell tumour of bone: a comprehensive review of pathogenesis, diagnosis, and treatment. Cureus 2023; 15: e46945.
[5] Brecher ME, Franklin WA and Simon MA. Immunohistochemical study of mononuclear phagocyte antigens in giant cell tumor of bone. Am J Pathol 1986; 125: 252-257.
[6] Szendröi M. Giant-cell tumour of bone. J Bone Joint Surg Br 2004; 86: 5-12.
[7] Amanatullah DF, Clark TR, Lopez MJ, Borys D and Tamurian RM. Giant cell tumor of bone. Orthopedics 2014; 37: 112-120.
[8] Wülling M, Engels C, Jesse N, Werner M, Delling G and Kaiser E. The nature of giant cell tumor of bone. J Cancer Res Clin Oncol 2001; 127: 467-474.
[9] Saxena CC, Safaya R, Kawatra Madan N, Khan SA and Iyer VK. Histopathological, immunohistochemical, and image analytic parameters characterizing the stromal component in primary and recurrent giant cell tumor of bone. J Clin Orthop Trauma 2016; 7: 109-114.
[10] Castiella T, Iruzubieta P, Monleón E, Cardiel MJ, Gómez-Vallejo J, Monzón M and Junquera MC. Stromal cells of giant cell tumor of bone show primary cilia in giant cell tumor of bone. Microsc Res Tech 2022; 85: 1065-1074.
[11] Nowell PC. The clonal evolution of tumor cell populations. Science 1976; 194: 23-28.
[12] Delabesse E, Oksenhendler E, Lebbé C, Vérola O, Varet B and Turhan AG. Molecular analysis of clonality in Kaposi's sarcoma. J Clin Pathol 1997; 50: 664-668.
[13] LYON MF. Sex chromatin and gene action in the mammalian X-chromosome. Am J Hum Genet 1962; 14: 135-148.
[14] Moore LD, Le T and Fan G. DNA methylation and its basic function. Neuropsychopharmacology 2013; 38: 23-38.
[15] Robert Finestra T and Gribnau J. X chromosome inactivation: silencing, topology and reactivation. Curr Opin Cell Biol 2017; 46: 54-61.
[16] Tan X, Zhang Y, Wei D, Yang Y and Xiang F. Denosumab for giant cell tumors of bone from 2010 to 2022: a bibliometric analysis. Clin Exp Med 2023; 23: 3053-3075.
[17] Chinder PS, Hindiskere S, Doddarangappa S and Pal U. Evaluation of local recurrence in giant-cell tumor of bone treated by neoadjuvant denosumab. Clin Orthop Surg 2019; 11: 352-360.
[18] Hayashida K, Kawabata Y, Kato I, Kamiishi T, Matsuo K, Takeyama M and Inaba Y. Clinical and pathological analysis of giant cell tumor of bone with denosumab treatment and local recurrence. J Orthop Sci 2022; 27: 215-221.
[19] Wessel LE, Strike SA, Singh A, Bernthal NM and Athanasian EA. The role of denosumab in the treatment of primary tumors of bone. J Hand Surg Am 2023; 48: 923-930.
[20] Mitjavila-Garcia MT, Bonnet ML, Yates F, Haddad R, Oudrhiri N, Féraud O, Magniez A, Makhlouf M, Vallot C, Rougeulle C, Bennaceur-Griscelli A and Turhan AG. Partial reversal of the methylation pattern of the X-linked gene HUMARA during hematopoietic differentiation of human embryonic stem cells. J Mol Cell Biol 2010; 2: 291-298.
[21] Rabkin CS, Janz S, Lash A, Coleman AE, Musaba E, Liotta L, Biggar RJ and Zhuang Z. Monoclonal origin of multicentric Kaposi's sarcoma lesions. N Engl J Med 1997; 336: 988-993.
[22] Wang W, Zhu H, Wang J, Wang S, Wang D, Zhao J and Zhu H. Clonality assessment of adenomatoid tumor supports its neoplastic nature. Hum Pathol 2016; 48: 88-94.
[23] Moniz S, Catarino AL, Marques AR, Cavaco B, Sobrinho L and Leite V. Clonal origin of nonmedullary thyroid tumours assessed by nonrandom X-chromosome inactivation. Eur J Endocrinol 2002; 146: 27-33.
[24] Feng W, He M, Jiang X, Liu H, Xie T, Qin Z, Huang Q, Liao S, Lin C, He J, Xu J, Ma J, Liu Y and Wei Q. Single-cell RNA sequencing reveals the migration of osteoclasts in giant cell tumor of bone. Front Oncol 2021; 11: 715552.
[25] Liu S, Ye F, Li D, He C, He H and Zhang J. p62 overexpression promotes neoplastic stromal cell proliferation and is associated with the recurrence of giant cell tumor of bone. Oncol Lett 2020; 20: 86.
[26] Court AC, Vega-Letter AM, Parra-Crisóstomo E, Velarde F, García C, Ortloff A, Vernal R, Pradenas C, Luz-Crawford P, Khoury M and Figueroa FE. Mitochondrial transfer balances cell redox, energy and metabolic homeostasis in the osteoarthritic chondrocyte preserving cartilage integrity. Theranostics 2024; 14: 6471-6486.
[27] Chen X, Ye F, He H, Chen G, Chen Z, Ye E, He B, Yang Y and Zhang J. Denosumab induces neoplastic stromal cell apoptosis *via* p62 downregulation dependent on autophagy pathway in giant cell tumour of bone. Curr Cancer Drug Targets 2024; 24: 565-578.
[28] Schubert A, Brockmeyer P, Kauffmann P, Wiegel J, Lautenbacher F, Miosge N and Schminke B. Alterations of bone proteins in medication-related osteonecrosis of the jaw. Eur J Oral Sci 2025; 133: e70003.
[29] Komori T. Regulation of proliferation, differentiation and functions of osteoblasts by runx2. Int J Mol Sci 2019; 20: 1694.
[30] Kelly JD, Haldeman BA, Grant FJ, Murray MJ, Seifert RA, Bowen-Pope DF, Cooper JA and Kazlauskas A. Platelet-derived growth factor (PDGF) stimulates PDGF receptor subunit di-

merization and intersubunit trans-phosphorylation. J Biol Chem 1991; 266: 8987-8992.
[31] Evans EK, Gardino AK, Kim JL, Hodous BL, Shutes A, Davis A, Zhu XJ, Schmidt-Kittler O, Wilson D, Wilson K, DiPietro L, Zhang Y, Brooijmans N, LaBranche TP, Wozniak A, Gebreyohannes YK, Schöffski P, Heinrich MC, DeAngelo DJ, Miller S, Wolf B, Kohl N, Guzi T, Lydon N, Boral A and Lengauer C. A precision therapy against cancers driven by *KIT/PDGFRA* mutations. Sci Transl Med 2017; 9: eaao1690.
[32] Duan Y, Haybaeck J and Yang Z. Therapeutic potential of PI3K/AKT/mTOR pathway in gastrointestinal stromal tumors: rationale and progress. Cancers (Basel) 2020; 12: 2972.
[33] Miller IJ, Blank A, Yin SM, McNickle A, Gray R and Gitelis S. A case of recurrent giant cell tumor of bone with malignant transformation and benign pulmonary metastases. Diagn Pathol 2010; 5: 62.
[34] Quatman CE, Alexander JH, Wakely PE Jr and Mayerson JL. Transformation of benign giant cell tumor of bone into epithelioid angiosarcoma. Am J Orthop (Belle Mead NJ) 2017; 46: E463-E467.
[35] Masui F, Ushigome S and Fujii K. Giant cell tumor of bone: an immunohistochemical comparative study. Pathol Int 1998; 48: 355-361.
[36] Schwartz HS, Eskew JD and Butler MG. Clonality studies in giant cell tumor of bone. J Orthop Res 2002; 20: 387-390.
[37] Raskin KA, Schwab JH, Mankin HJ, Springfield DS and Hornicek FJ. Giant cell tumor of bone. J Am Acad Orthop Surg 2013; 21: 118-126.
[38] Pulford KA, Rigney EM, Micklem KJ, Jones M, Stross WP, Gatter KC and Mason DY. KP1: a new monoclonal antibody that detects a monocyte/macrophage associated antigen in routinely processed tissue sections. J Clin Pathol 1989; 42: 414-421.
[39] Wülling M, Delling G and Kaiser E. The origin of the neoplastic stromal cell in giant cell tumor of bone. Hum Pathol 2003; 34: 983-993.
[40] Ghert M, Simunovic N, Cowan RW, Colterjohn N and Singh G. Properties of the stromal cell in giant cell tumor of bone. Clin Orthop Relat Res 2007; 459: 8-13.
[41] Athanasou NA, Bliss E, Gatter KC, Heryet A, Woods CG and McGee JO. An immunohistological study of giant-cell tumour of bone: evidence for an osteoclast origin of the giant cells. J Pathol 1985; 147: 153-158.
[42] Joyner CJ, Quinn JM, Triffitt JT, Owen ME and Athanasou NA. Phenotypic characterisation of mononuclear and multinucleated cells of giant cell tumour of bone. Bone Miner 1992; 16: 37-48.
[43] Wang ZZ, Wang K, Xu LF, Su C, Gong JS, Shi JS, Ma XD, Xie N and Qian JY. Unlocking the potential of collagenases: structures, functions, and emerging therapeutic horizons. Biodes Res 2024; 6: 0050.
[44] French MF, Mookhtiar KA and Van Wart HE. Limited proteolysis of type I collagen at hyperreactive sites by class I and II Clostridium histolyticum collagenases: complementary digestion patterns. Biochemistry 1987; 26: 681-687.
[45] Taylor EL and Westendorf JJ. Histone mutations and bone cancers. Adv Exp Med Biol 2021; 1283: 53-62.
[46] Lüke J, von Baer A, Schreiber J, Lübbehüsen C, Breining T, Mellert K, Marienfeld R, Schultheiss M, Möller P and Barth TFE. H3F3A mutation in giant cell tumour of the bone is detected by immunohistochemistry using a monoclonal antibody against the G34W mutated site of the histone H3.3 variant. Histopathology 2017; 71: 125-133.
[47] Lau CP, Huang L, Wong KC and Kumta SM. Comparison of the anti-tumor effects of denosumab and zoledronic acid on the neoplastic stromal cells of giant cell tumor of bone. Connect Tissue Res 2013; 54: 439-449.
[48] Mak IW, Evaniew N, Popovic S, Tozer R and Ghert M. A translational study of the neoplastic cells of giant cell tumor of bone following neoadjuvant denosumab. J Bone Joint Surg Am 2014; 96: e127.
[49] Smrke A, Gennatas S, Huang P and Jones RL. Avapritinib in the treatment of PDGFRA exon 18 mutated gastrointestinal stromal tumors. Future Oncol 2020; 16: 1639-1646.
[50] Le N, Chen J, Ekert PG, Brown LM and Manoharan N. PDGFRA in paediatric high-grade glioma - target or distraction? Neoplasia 2025; 69: 101231.
[51] Mahdal M, Neradil J, Mudry P, Paukovcekova S, Staniczkova Zambo I, Urban J, Macsek P, Pazourek L, Tomas T and Veselska R. New target for precision medicine treatment of giant-cell tumor of bone: sunitinib is effective in the treatment of neoplastic stromal cells with activated PDGFRβ signaling. Cancers (Basel) 2021; 13: 3543.
[52] Rascio F, Spadaccino F, Rocchetti MT, Castellano G, Stallone G, Netti GS and Ranieri E. The pathogenic role of PI3K/AKT pathway in cancer onset and drug resistance: an updated review. Cancers (Basel) 2021; 13: 3949.
[53] Zhang J, Yu XH, Yan YG, Wang C and Wang WJ. PI3K/Akt signaling in osteosarcoma. Clin Chim Acta 2015; 444: 182-192.

Supplementary Table 1. *HUMARA* polymorphisms and Cell Clonality of 32 GCTB patients

Sample No.	*HUMARA*	Clonality of Multinucleated Giant Cell	Clonality of CD68-negative Spindle Cell	Sample No.	*HUMARA*	Clonality of Multinucleated Giant Cell	Clonality of CD68-negative Spindle Cell
1	Homozygous	NA	NA	17	Heterozygous	Polyclonal	Monoclonal
2	Homozygous	NA	NA	18	Homozygous	NA	NA
3	Homozygous	NA	NA	19	Heterozygous	Polyclonal	Monoclonal
4	Homozygous	NA	NA	20	Heterozygous	Polyclonal	Monoclonal
5	Heterozygous	Polyclonal	Monoclonal	21	Homozygous	NA	NA
6	Homozygous	NA	NA	22	Heterozygous	Polyclonal	Monoclonal
7	Homozygous	NA	NA	23	Homozygous	NA	NA
8	Homozygous	NA	NA	24	Heterozygous	Polyclonal	Monoclonal
9	Heterozygous	Polyclonal	Monoclonal	25	Heterozygous	Polyclonal	Monoclonal
10	Heterozygous	Polyclonal	Monoclonal	26	Homozygous	NA	NA
11	Homozygous	NA	NA	27	Homozygous	NA	NA
12	Homozygous	NA	NA	28	Heterozygous	Polyclonal	Monoclonal
13	Homozygous	NA	NA	29	Homozygous	NA	NA
14	Homozygous	NA	NA	30	Homozygous	NA	NA
15	Homozygous	NA	NA	31	Heterozygous	Polyclonal	Monoclonal
16	Homozygous	NA	NA	32	Homozygous	NA	NA

NA: not available; *HUMARA*: human androgen receptor gene; GCTB: giant cell tumor of bone.